Journal of Sciences, Islamic Republic of Iran 29(2): 143 - 156 (2018) http://jsciences.ut.ac.ir
University of Tehran, ISSN 1016-1104

Estimation of Plunge Value in Single- or Multi-Layered Anisotropic Media Using Analysis of Fast Polarization Direction of Shear Waves

K. Latifi[1], A. Sadidkhouy[2], and M. R. Ghassemi[*1]

[1]*Research Institute for Earth Sciences, Geological Survey of Iran (GSI), Tehran, Islamic Republic of Iran*
[2] *Deportment of Seismology, Institute of Geophysics, Faculty of Sciences, University of Tehran, Tehran, Islamic Republic of Iran*

Received: 28 July 2016 / Revised: 22 December 2016 / Accepted: 21 February 2017

Abstract

Estimation of the fast polarization direction of shear seismic waves that deviate from horizontal axis is a valuable approach to investigate the characteristics of the lower crust and uppermost mantle structures. The lattice preferred orientation of crystals, which is generally parallel to the downward or upward flow of the mantle or crust, is an important reason for the occurrence of fast axis plunge in these structures. We introduce a new method to estimate the plunge and the true percent of anisotropy. To evaluate the accuracy of the method, we applied it to back azimuthal synthetic receiver functions produced by the Raysum code. The output resulted from this new method (including plunge and percent of anisotropy) were compared with inputs of Raysum code, and reveal that there is a very good coherence among the inputs and output values estimated by our method. This method has been applied to anisotropy analysis beneath two different stations of SHGR in Iran and MOX in Germany. The splitting parameters beneath the SHGR station, are estimated to be $\varphi=60\pm1$ degrees and $\delta t=0.54\pm0.02$ sec. The plunge value and percentage of anisotropy in SHGR are estimated to be 45 ± 0.5 degrees and 4 percent, which can correspond to an old flow in a subduction zone within the area. The splitting parameters in the crust beneath the MOX station, are estimated as $\varphi=98\pm2$ degrees and $\delta t=0.38\pm0.02$ sec. The plunge value and percentage of anisotropy in the crust of the MOX are estimated 45 ± 0.2 degrees and 5.5%.

Keywords: Anisotropy; Fast polarization direction; Fast axis plunge estimation; Shear wave splitting; Receiver functions.

Introduction

Some physical properties such as the density of a material, have an independent value for direction; they are therefore scalar properties. However, some properties such as wave velocity in crystallized materials are generally dependent on direction [1, 2, and 3]. Non-directional properties, such as density, can be specified by a single number. This is a scalar property or zero rank tensor. But directional properties such as

* Corresponding author: Tel: +982164592476; Fax: +982166070511; Email: m.r.ghassemi@ries.ac.ir

wave velocity can't be specified by a single number. They are vector or tensor property [3]. If a physical property involving two vectors were measured, it wouldn't vary with orientation within the material; i.e. material is isotropic. On the contrary, the crystalline materials are commonly anisotropic because physical characteristics such as wave velocity depends on crystals lattice preferred orientation [1, 2]. Seismic anisotropy indicates the variation of the seismic wave velocity with respect to its propagation direction [4]. Seismic anisotropy can detect a wide range of alignments including cracks, micro-fractures, mineral crystallography, layers, etc. [1, 3]. An important mode of anisotropy occurs in homogeneous materials [5]. For example, minerals such as olivine and quartz are individually homogeneous. However, according to crystallographic structures of the minerals, the seismic waves pass them with different velocities in certain directions [6]. Rock material in the crust and mantle includes mineral aggregates in which individual mineral crystals are randomly oriented before deformation [7]. After deformation in a crystal-plastic manner, specific crystallographic axes become oriented almost parallel to the ductile flow direction of the rock material [8]. This process results in "lattice preferred orientation" (LPO) [1, 2]. The lattice preferred orientation of olivine crystals in large strain, is parallel to the ductile shear direction; therefore, the fast polarization direction should have the same direction [9, 10, 2]. The mineral alignments are usually deviated from the horizontal pose in the uppermost mantle of the subduction zones [11]. Since fast direction in the upper mantle is parallel to mineral alignments [9, 10, 2], it is possible that the fast axis makes a plunge angle with horizon in the subduction zones or convection cells, (Fig. 1). The plunge value offers good approximations of true magnitudes regarding the anisotropy (percentage of anisotropy) [11]. The plunge estimation is useful for obtaining some information about anisotropic structures in the crustal layers and the upper mantle. The dip value of the aligned minerals or melt inclusions of the anisotropic shear zones could be well estimated by obtaining the plunge value [11, 12]. Estimation of fast axis plunge in the upper mantle is an important approach to study the situation of recent tectonic framework of different regions. Ability in finding plunge angle is also very important for geodynamic interpretation of surface-recorded waveform effects [11]. Therefore, resolving the fast axis plunge has been among the typical problems in seismology over the past two decades. Contrary to our technique, the previous methods focus on forward modeling to achieve plunge angle assessments [12, 13, 14]. This article presents a new technique based on combination of inversion and forward modeling methods, which can estimate seismic anisotropy parameters with respect to the deviation of fast polarization directions from the horizontal axis, which is in fact the plunge of the polarization direction.

In this study, the technique was applied to estimate splitting parameters plus the plunge value in a single anisotropic layer. Then, the approximations were transformed into multi anisotropic layers. Some experiments that use synthetic and real data were applied here to check the current method so as to determine the plunge value.

a) Estimation of splitting parameters

According to the method used by Nagaya et al. [15], Liu and Niu [16] and modified by Rümpker et al. [17], the maximum amplitude of azimuthal Ps phases, situated on a poorly anisotropic case, is fitted to a cosine quadratic four-lobed pattern as cos [2(θ-φ)], in which θ

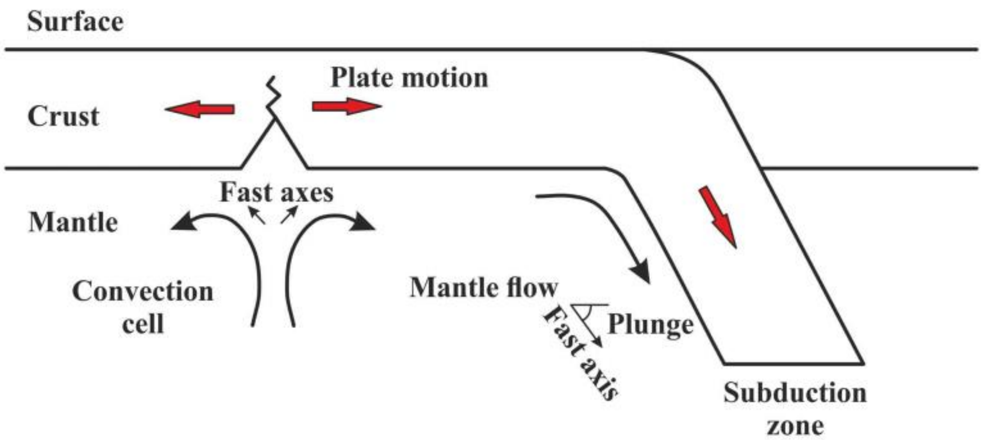

Figure 1. The cartoon scheme illustrating fast axis plunge in convection cells and subduction zone.

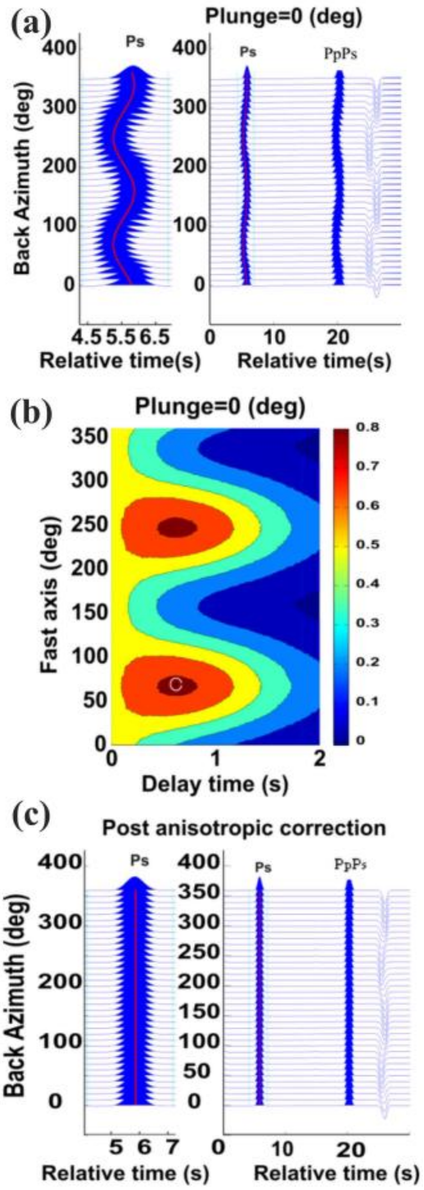

Figure 2. a) Synthetic Radial receiver-functions are sorted as a function of back-azimuth relevant to model 1a. The red line shows the harmonic pattern of Ps phases' arrival times. It is zoomed on the left. b) Splitting parameters estimated by the Ruempker et al.'s [17] technique. The white circle is standard deviation and the black point at the center of this circle indicates maximum stacking of Ps amplitudes fitting to red harmonic pattern showed in (a). The splitting parameters related to this black point leads into the best results. c) Synthetic radial receiver-functions plotted as a function of back-azimuth, followed by anisotropic correction. The harmonic azimuthal Ps pattern is changed to a line by the anisotropic correction. The harmonic azimuthal Ps pattern is changed into a line after correcting the receiver functions for splitting parameters of the layer.

is back azimuth and φ is fast direction. Rümpker et al. [17] applied a new stacking technique so as to estimate splitting parameters (δt, φ) by a cosine quadratic equation which will be studied in detail further forward. They used Raysum code devised by Frederiksen and Bostock [18] to make synthetic receiver functions. Rümpker's technique shows how cos [2(θ-φ)] leads to the azimuthal variation of the effective arrival time for the weakly anisotropic medium — that is 't_e' — as the harmonic move-out (Fig. 2a and Table 1, model 1a), which can be obtained as follows [17]:

$$t_e(\theta) = t_0 + dt = t_0 - \frac{\delta t}{2}\cos[2(\theta - \varphi)] \qquad (1)$$

Where t_0 is the isotropic arrival time (sec), θ is back azimuth (deg) and dt (sec) represents the (azimuthal) move-out with respect to t_0. The fast polarization direction φ and split time δt (in the radial component of the receiver functions) can be estimated by applying the harmonic pattern stacking analysis on receiver functions. The analysis involves a grid search for splitting parameters according to the stacking of Ps phase amplitudes which are fitted into harmonic patterns. Accordingly, the maximum value in this grid search becomes a feasible result (Fig. 2b).

b) Estimation of plunge angle and its effect on back azimuthal receiver function

As a total effect of plunge in anisotropic layers, we can obtain the corresponding apparent splitting parameters first by resolving the splitting parameters of the layer from the analysis of the *Ps* phase (just as in the single-layer case described in (a)). Once these splitting parameters are known, we can remove the effects of the anisotropy from Ps phases in receiver functions. The harmonic azimuthal Ps pattern is modified to align with the anisotropic correction (Fig. 2c). We apply the correction to both the radial and the transverse component: The splitting effect of the layer is first removed by transforming the radial and transverse components into the corresponding fast-slow coordinate system (given by φ) and, then, the two traces are shifted (each by δt/2) before back transformation into the radial-transverse coordinates. The new harmonic cosine pattern is recognized in azimuthal Ps phases in radial components after the anisotropic correction, if the fast axis is inclined or in other words, the fast direction have plunge [Table 1, Model 1b; Fig. 3c]. This new harmonic pattern denotes the arrival times of Ps phases in radial receiver functions which are dependent on the back azimuth of receiver functions. Figure 3c shows a two-lobed pattern which have been related to the variation of arrival times in the maximum amplitude of Ps converted

Table 1. Input models related to models 1 and 2. The half space is marked by zero in the first column.

Thickness (m)	Vp (m/s)	Vs (m/s)	isotropic	%P	%P	φ (deg)	Plunge (deg)
Model 1a							
Thickness (m)	Vp (m/s)	Vs (m/s)	isotropic	%P	%P	φ (deg)	Plunge (deg)
50000	6700	3868	0	4	4	70	0
0	8500	4907	1	0	0	0	0
Model 1b							
Thickness (m)	Vp (m/s)	Vs (m/s)	isotropic	%P	%P	φ (deg)	Plunge (deg)
50000	6700	3868	0	4	4	70	50
0	8500	4907	1	0	0	0	0
Model 2							
Thickness (m)	Vp (m/s)	Vs (m/s)	isotropic	%P	%P	φ (deg)	Plunge (deg)
35000	6500	3753	0	3	3	70	40
30000	7800	4503	0	3	3	30	50
0	9200	5312	1	0	0	0	0

Table 2. Output data related to Table 1 which are estimated by forward modeling. The last two rows are for two anisotropic layers in Model 2.

Models' outputs	**¨ (deg)**	**Std ¨**	**dt (sec)**	**Std dt**	**Plunge (deg)**	**Std plunge**	**Real anisotropy (P & S)**
Model 1a	70	10.0	0.54	0.08	0	-	4.0 %
Model 1b	70	8.3	0.52	0.08	50	1.0	4.0 %
Model 1b*	70	5.0	0.52	0.07	55	3.0	4.0 %
Model 1b**	68	1.0	0.44	0.01	50	1.0	3.5 %
Model 1b***	64	2.0	0.54	0.01	55	1.2	4.0 %
Model 2	70	2.0	0.26	0.02	40	0.6	3.0 %
	22	2.0	0.26	0.08	60	2.5	2.5 %

* With random noise; ** Random selection; *** Noise added to random selection

phases. These are indicated by the first degree of the cosine function. Accordingly, by testing particularly poor anisotropic layers, the empirical equation for the pattern of Ps phases is derived as follows:

$$t_{e2}(\theta) = t_0 + dt = t_0 + \frac{\delta t_2}{2}\cos[(\theta - \varphi)] \qquad (2)$$

Where t_{e2} is the harmonic move-out in the new cosine pattern (Fig. 3c), dt explains the sinusoidal move-out with respect to t_0 (sec), the delay time value, δt_2, obtained from Eq. (2), is a new delay time (different from the split time). The fast direction and new delay time are estimated by determining the cosine curve function which is designed to fit to maximum azimuthal Ps phases of amplitudes.

For this assumption, a new grid search computed by stacking all radial receiver functions can be measured in terms of a maximum value pertaining to the contour diagrams, following the anisotropic corrections, φ and δt_2 (Fig. 3d). In this recent hypothesis, the fast direction deviation from horizontal (i.e. the plunge angle) is determined using back azimuthal receiver functions. In this approaches, the plunge angle determines in three steps: (a) splitting parameters which are estimated by the Rümpker et al. [17] method, (b) anisotropic correction which is followed by finding the new harmonic pattern via common methods [17], (c) estimating the plunge by forward modeling via synthetic models.

The method that was devised by Frederiksen and Bostock [18] is applied to make synthetic radial receiver functions. The forward modeling is carried out to estimate the best model and make synthetic receiver functions similar to the real ones. In this way, azimuthal patterns for Ps phases were used before and after anisotropic correction so as to estimate two variables, i.e. δt and δt_2 similar to those observed ones in an anisotropic layer. Thereby a synthetic model with the least squared value was obtained from the approved model. The least squared value was derived as follows:

$$Ls = \sqrt{\Sigma\left[(X_O - X_S)^2\right]} \qquad (3)$$

Where X_O is the observed parameters i.e. δto; δt_2o and X_S is the parameters of the synthetic models, i.e. δt_S and δt_{2S}. Eq. (3) can be changed as follows:

$$Ls = \sqrt{\left[(\delta t_O - \delta t_S)^2 + (\delta t_{2O} - \delta t_{2S})^2\right]} \qquad (4)$$

The minimum value for the last equation is the favorable response. The synthetic model closest to the

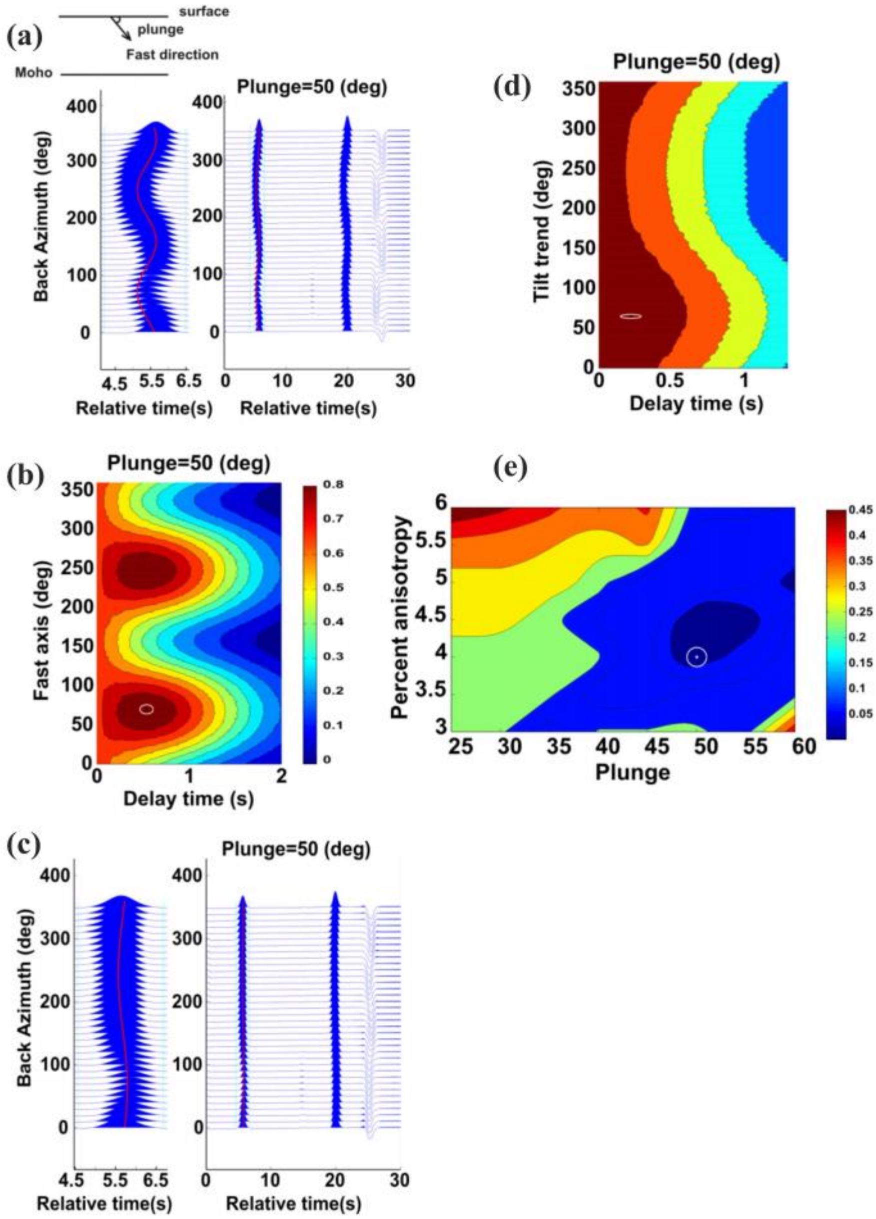

Figure 3. a) Synthetic Radial receiver-functions sorted as function of back-azimuth relevant to model 1b. The red line shows the harmonic pattern of Ps phases arrival times and it zoomed at left. b) The splitting parameters estimated by the Ruempker et al.'s [17] technique. The maximum value of this contour diagram (at the center of white circle) is relevant to stacking of maximum Ps phases amplitudes fitted to the red curve illustrated in (c), which shows fast direction (φ) and split time (δt). c) Synthetic radial receiver-functions plotted as a function of back-azimuth, followed by anisotropic correction. The four-lobed harmonic azimuthal Ps pattern with 180° period shown in (a), is changed to a new two-lobed harmonic pattern with 360° period, by anisotropic correction. d) Contour diagrams computed by fitting the best harmonic curve to maximum amplitudes of Ps phases based on Eq. (3), which shows fast direction (φ) and secondary split time (δt_2). e) Contour diagram drawn using forward modeling based on Frederiksen et al.'s [18] method. The minimum value of this contour diagram shows plunge value and real percent of anisotropy related to model 1b. The white circle is standard deviation.

real-world case was created by a grid search illustrated in Fig. 3e. The plunge value and true percentage of anisotropy are shown in this grid search.

1. Influence of the plunge on synthetic data

Several cases are examined to estimate the efficiency and accuracy of the method. In the present study, the focus was on three main objectives: a) estimating the apparent splitting parameters of a plunge-bearing anisotropic layer using radial components related to the receiver functions, b) estimating the plunge angle and its azimuth, c) evaluating the plunge effect on the actual anisotropy, and estimating the actual percentage of the anisotropy. In this way, some different models were examined and synthetic seismograms were computed by the ray tracing method of Frederikson and Bostock [18]. The velocity models used in the synthetic assays are listed in Table 1. They were comprised of: 1) one anisotropic medium with a single plunge angle, 2) one anisotropic medium with a wide range of plunge angles and percent of anisotropy, and 3) two anisotropic layers with different plunge angles.

a. The one-layered anisotropic model

According to the previous comments, synthetic seismograms were computed in accordance with model 1a. and model 1b in Table 1. The model 1a was related to a one layered anisotropic crustal model wherein the fast direction was horizontal. The results of splitting parameters had been estimated by Rümpker et al. [17]; they are listed in Table 2. Model 1b was also a one-layered anisotropic crustal model with a fast direction that deviated from horizon. The splitting parameters estimated by the current method are listed in Table 2. It is clear in this case that the magnitude of anisotropy, i.e. split time, is 0.52 seconds which is a little lower compared to the case wherein the fast direction was horizontal. The pattern for Ps phases (back azimuthal of receiver functions) is related to model 1b which is illustrated in Fig. 3a. The splitting parameters were estimated in a grid search which is illustrated in Fig. 3b. The azimuthal pattern for Ps phases was converted into a first degree cosine curve, after the anisotropic correction had taken place. This is illustrated in Fig. 3c. Also, the secondary delay time, i.e. δt_2 and tilt trend were estimated by the relevant stacking method (Fig. 3d). Their values are listed in Table 2. It is evident from Fig. 3d and Fig. 3b that the trend of the plunge is the same as the fast polarization direction. Just like the fast polarization direction value, the tilt trend value indicates the plunge accuracy in the anisotropic media. Afterwards, the plunge value and actual percentage of the anisotropy were estimated by a grid search for forward modeling which is illustrated in Fig. 3e. As can be seen, the plunge estimated by the method of forward modeling is actually very similar to the assumed model [model 1b in Table1], which was obtained classically. To determine the effect of noise on the results, the same model was applied in the manner described earlier. However, in this case, noise was added to synthetic data (Fig. 4a-c). And yet in another case, random selection was tested and noise was added to a set of randomly selected data, (Figs. 5a-c and Figs. 6a-c, respectively). The output is listed in Table 2.

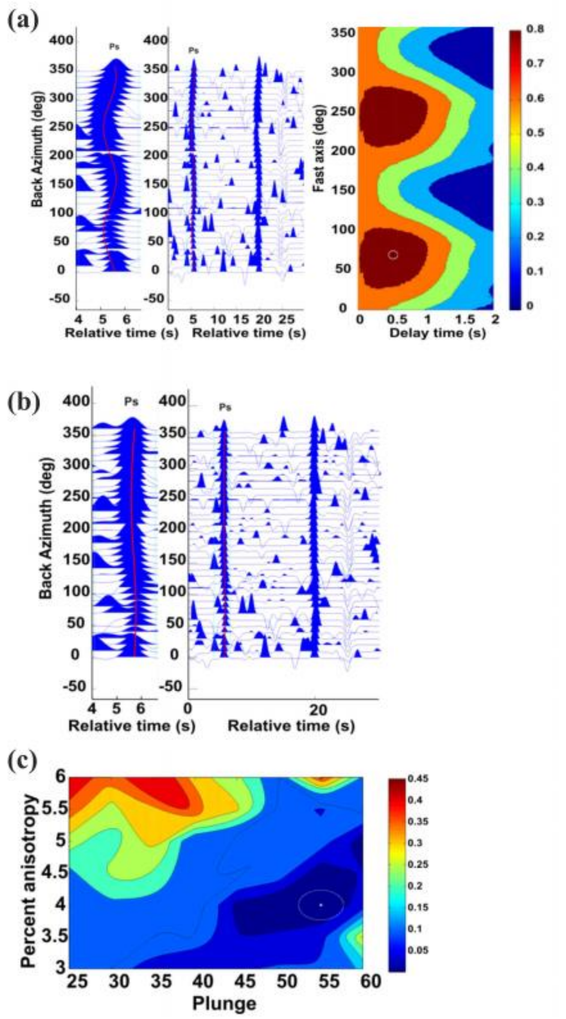

Figure 4. Effect of random noise in receiver functions on the Ps-splitting analysis and estimation of plunge angle using radial component stacking in a single-layer case (model 1b and Table1). a) Noise randomly added to the synthetic radial receiver-functions which is sorted as a function of back-azimuth relevant to model 1b. The red line indicates harmonic pattern of Ps phases of arrival times and it is zoomed at the left. The contour diagram shows splitting parameters related to the model 1b. b) Synthetic radial receiver-functions are plotted as functions of back-azimuth, followed by anisotropic correction. c) Contour diagram drawn by forward modeling based on Frederiksen et al.'s [18] method. The minimum value in this contour diagram shows plunge value and real percent of anisotropy, relevant to model 1b, which is noise-bearing. As shown here, there is 5 degrees of error in the plunge value (see Table 2).

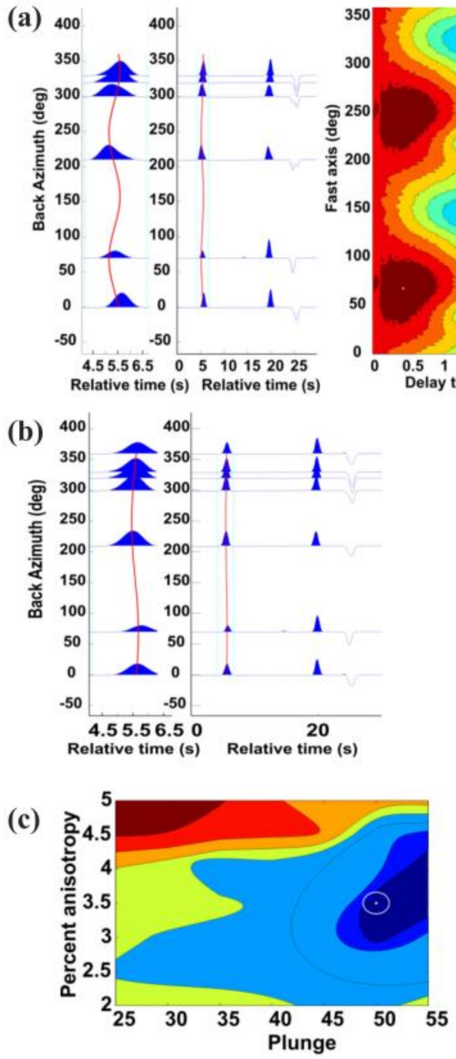

Figure 5. Effect of non-uniform distribution of receiver functions on the Ps-splitting analysis and estimation of plunge angle value using radial component stacking in a single-layer case (model 1b and Table1). a) This figure is similar to Fig 4 relevant to model 1b, however inputs of radial receiver-functions are randomly selected as a function of back-azimuth. b) Synthetic radial receiver-functions plotted as a function of back-azimuth, followed by anisotropic correction. c) Grid-search carried out for the plunge and real percent of anisotropy.

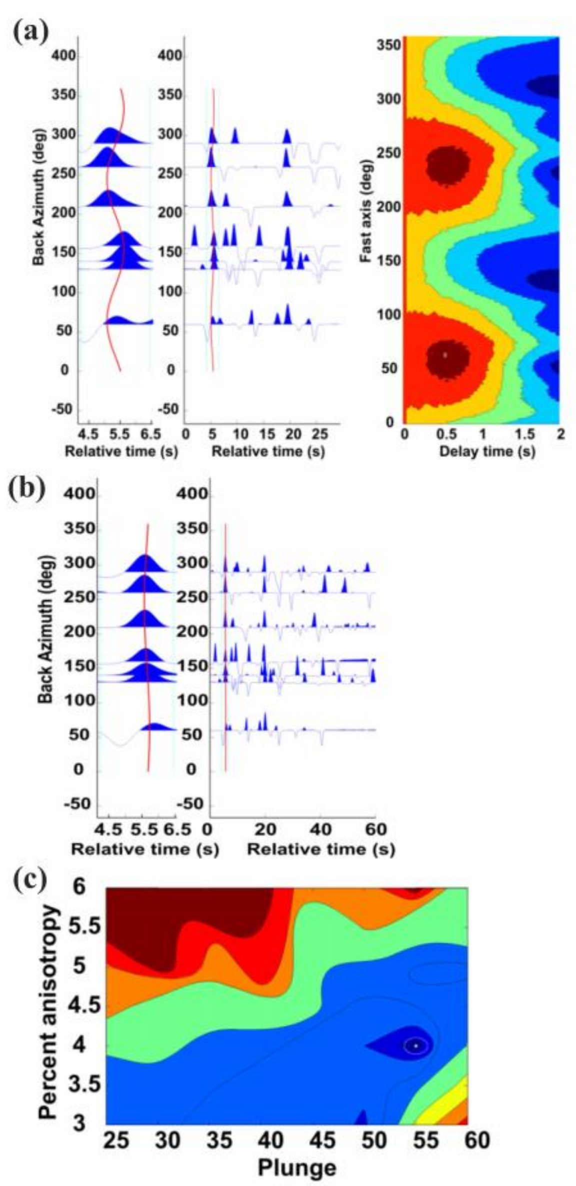

Figure 6. Descriptions are similar to those of Fig 5, however, the noise added to random selection of synthetic receiver-functions are relevant to model 1b.

b. One-layered anisotropic models with a wide range plunge angle and percent of anisotropy

The models with wide range of plunge angles and percents of anisotropy are used in our investigation to assess the accuracy of the method. Accordingly, the percent of anisotropy is firstly presumed to be constant, however the plunge angle is varied in a wide range from 30 to 70 degrees. The synthetic receiver functions made by Raysum code, are used as inputs for our method, and the outputs (plunge angle and true percent of anisotropy) which were estimated by this method should be comparable together. The processed data presented in Fig. 7, reveal that the input values including fast axis plunge and true percent of anisotropy are coherent with output values estimated by our method. Secondly, we assumed that the fast axis plunge is constant (50º) but percent of anisotropy could be variable. The processing and results have been presented in Fig. 8 and Tables 3

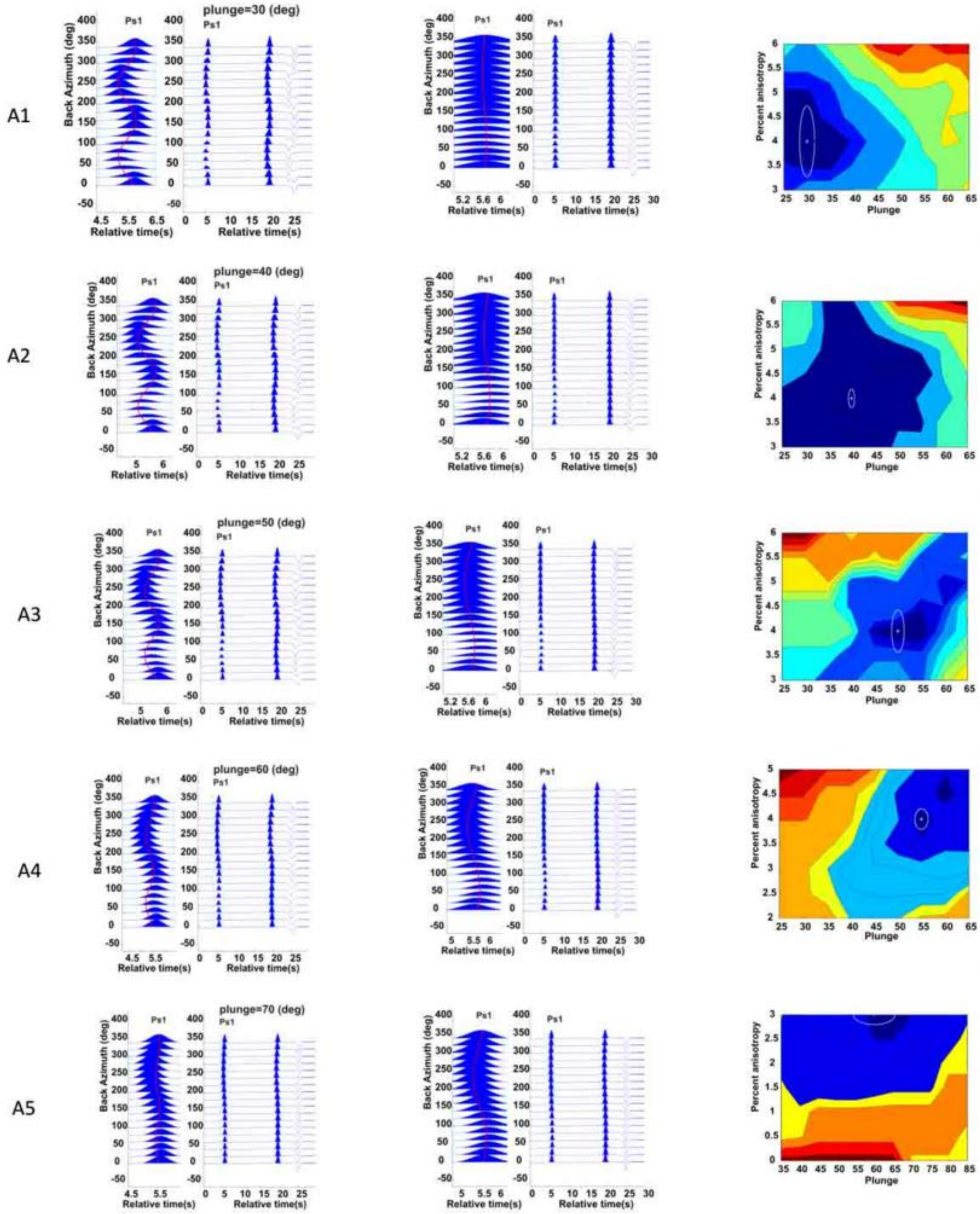

Figure 7. Fast polarization direction plunge and percent of anisotropy estimated using synthetic receiver functions related to one layered anisotropic models. For all of the models from A1 to A5, the thickness of layers are 50 kilometers and the percent of anisotropy are constant (4%), assuming that the azimuth of fast polarization directions are 70 degrees but the fast direction plunges are varied from 30º to 70º. Left) The back azimuthal receiver functions which are produced by Raysum code. The four-lobed curves are almost fitted to maximum Ps phases that are zoomed at left. Middle) The synthetic receiver function after anisotropic correction. As presented in these figures, the Ps phase patterns are changed from four-lobed curves to two-lobed curves. Right) The percent of anisotropy and fast direction plunge which are estimated using our method.

and 4.

c. Two-layered anisotropic model

The next model that was applied to measure the efficiency of this method was the two-layered anisotropic crustal model. The new model, however, correlated with two anisotropic layers with two different plunge angles. The input parameters of the synthetic

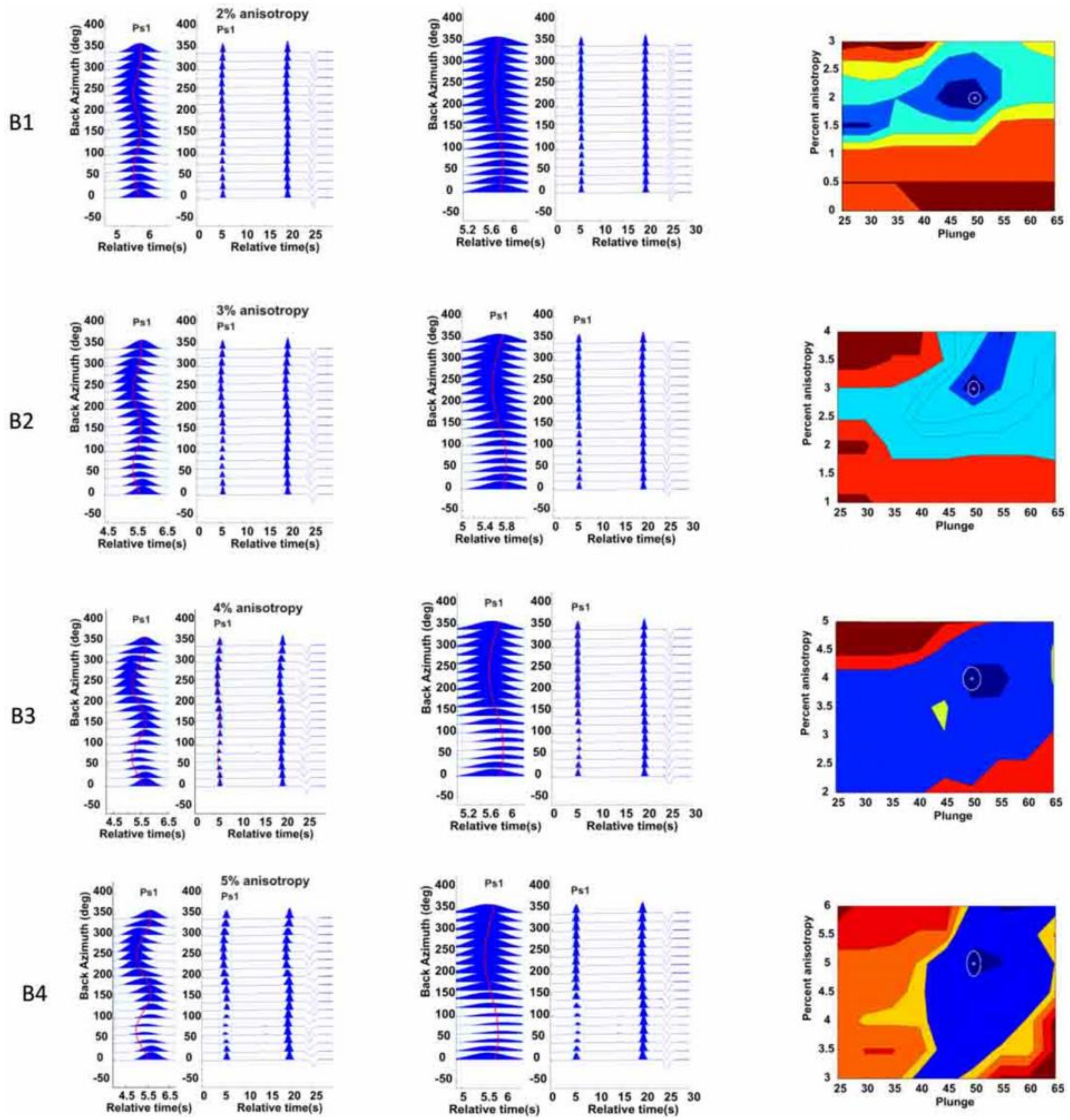

Figure 8. Captions similar to that of Fig. 7, except for plunge of the fast axis which is constant (50º) and percent of anisotropy, which varied between 2% to 5%.

model are listed in Table 1 (model 2). The splitting parameters and plunge angle — pertinent to the upper crust — were estimated in the same manner as the case for the one-layer anisotropic. Their results are listed in Table 2 [see Fig. 9]. Estimating the splitting parameters and plunge angle of the lower crust was feasible once the anisotropy was eliminated from the upper-crust. The splitting parameters and plunge of anisotropy in the lower layer could be estimated after correction. The procedure is shown in Fig. 9 and is further detailed in Table 2. The fast polarization direction and plunge angle in the upper-crust were estimated to be 70 degrees and 40 degrees. These parameters were estimated to be 22 degrees and 60 degrees in the lower-layer. There was a good harmony with the input synthetic model for the upper-layer, but there was less harmony regarding the lower layer. Therefore, this method was more useful for estimating the plunge value in just one anisotropic layer.

Table 3. Input and output values related to Fig. 7.

	Inputs						Outputs*	
Model	Thick. (m)	Vp (m/s)	Vs (m/s)	Fast direction (deg)	Plunge (deg)	Percent of anisotropy	Plunge (deg)	Percent of anisotropy
A1	50000	6700	3868	70	30	4%	30	4%
A2	50000	6700	3868	70	40	4%	40	4%
A3	50000	6700	3868	70	50	4%	50	4%
A4	50000	6700	3868	70	60	4%	55	4%
A5	50000	6700	3868	70	70	4%	60	3%

* by the method

Table 4. Input and output values related to Fig. 8.

	Inputs						Outputs*	
Model	Thick. (m)	Vp (m/s)	Vs (m/s)	Fast direction (deg)	Plunge (deg)	Percent of anisotropy	Plunge (deg)	Percent of anisotropy
B1	50000	6700	3868	70	30	2%	50	2%
B2	50000	6700	3868	70	40	3%	50	3%
B3	50000	6700	3868	70	50	4%	50	4%
B4	50000	6700	3868	70	60	5%	50	5%

* by the method

2. Data and data processing

In this section we describe the results of our technique as applied to real receiver functions in the SHGR (Shooshtar) station of Iranian National Seismic Network (INSN) and the MOX (Moxa) station in Germany (Institute for Geosciences of the Friedrich-Schiller-University Jena, Burgweg). These stations are of the broad band type, as shown in Fig. 10. The SHGR station is located in south of Zagros fold and thrust belt in Iran. Receiver functions were generated from three components of teleseismic earthquake records between 35° and 90°, with magnitudes more than 5. The radial receiver functions are shown in Fig. 11 as a function of back-azimuth. There were two Ps converted phases presumably related to Moho and a discontinuity in 23 kilometers under the Moho discontinuity. The first pattern for Ps phases was ignored in azimuthal receiver functions, while through the second pattern of Ps phases, the average values of two-layer splitting parameters can be estimated by Rümpker et al. [17] method (Fig. 11a). The plunge angle is measured by forward modeling based on the method developed by Frederiksen and Bostock [18]. The plunge value and true percentage of anisotropy were estimated by a grid search according to equation (4) that functions through the least square value to determine an approved model. The apparent fast polarization direction and delay time from the uppermost mantle to the surface beneath the SHGR station were estimated to be 60±1 degrees and 0.54±0.02 seconds. The plunge angle and percentage of anisotropy were also estimated to be 45±0.5 degrees and 4±0.1 percent [Table 5]. The receiver functions for the MOX station as a function of back-azimuth are illustrated in Fig. 12. The converted phases for the Moho Ps are evident in radial receiver functions. Since there was an excellent coverage of azimuthal receiver functions, the previous technique was a practicable approach for estimating the splitting parameters (Fig. 12). The plunge value could be estimated by stacking the new harmonic cosine pattern after correcting the anisotropy. This new periodic curve pattern was related to the plunge angle and tilt trend (the trend of plunge) (Fig. 12). The plunge value could be estimated by the previous forward modeling method based on creating a synthetic model, the properties of which were similar to the observed properties beneath the station. The splitting parameters were estimated by a grid search represented in Fig. 12, and their values were $\varphi = 98 \pm 2$ degrees and $\delta t = 0.38 \pm 0.02$ seconds. The plunge angle was measured in a grid search illustrated in Fig. 12. Its value was estimated to be 45 ± 2 degrees and the true percentage of anisotropy was 5.5 ± 0.3.

Results and Discussion

We investigated the shear-wave splitting effects of Ps converted phases from discontinuities beneath a receiving station. We demonstrated that the effective times of arrival for Ps phases of synthetic radial receiver functions varied depending on the back azimuth. Their effective arrival time variations versus θ (back azimuth) exhibited a four-lobed pattern [17]. The equation of this pattern, i.e. Eq. (1) had one dependent variable (t_e) and two independent variables, i.e. φ (fast direction) and δt (split time). We revealed that the splitting parameters could be estimated by stacking the pattern for azimuthal Ps phases. We investigated the inclination effect of the fast direction on the arrival times for Ps waves using

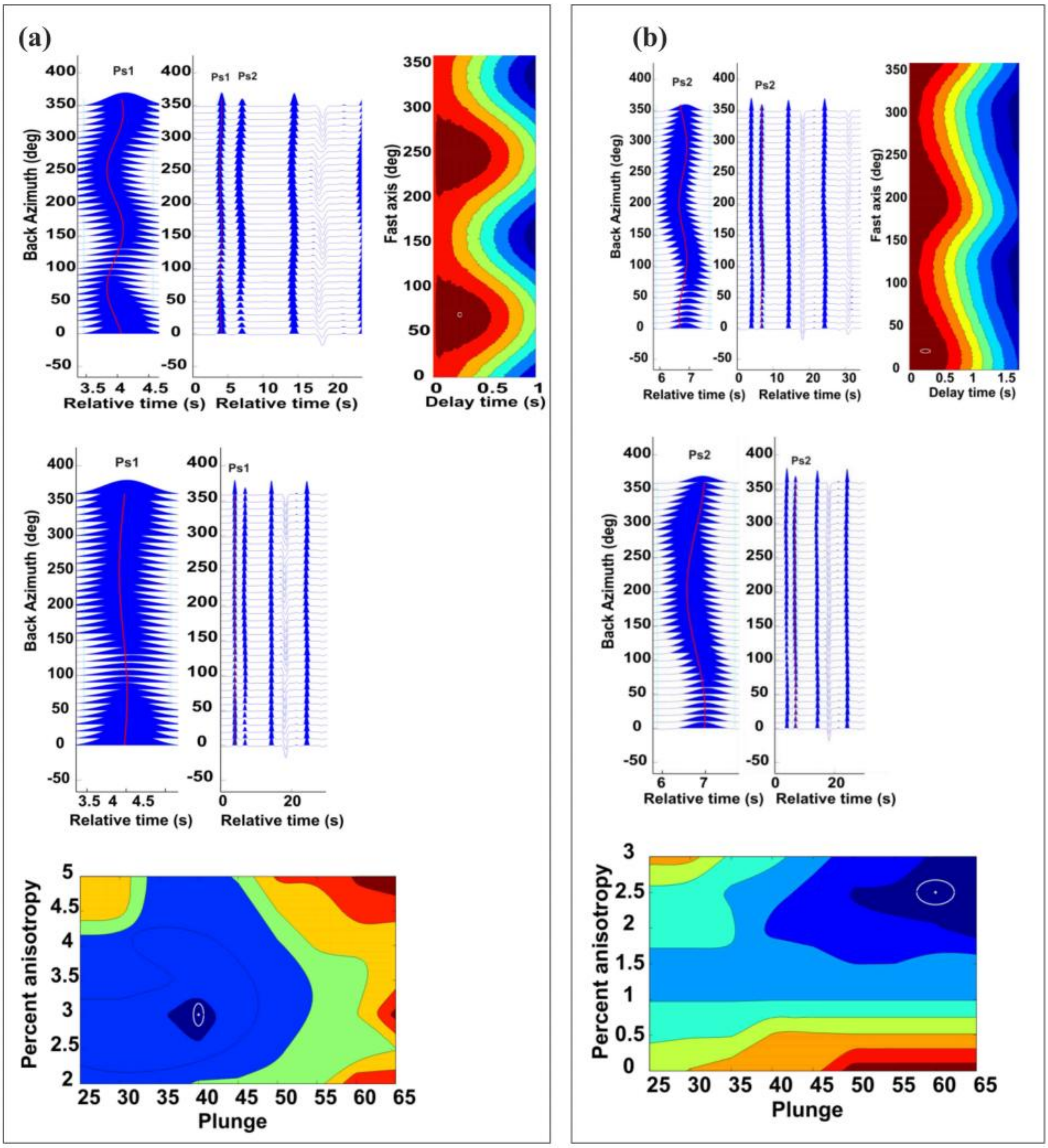

Figure 9. a) Receiver function splitting analysis for the upper layer of two anisotropic layers model (model 2; Table 1) Top) The synthetic receiver-functions as a function of back-azimuth relevant to a two-layered model (model 2). Middle) Synthetic radial receiver-functions plotted as a function of back-azimuth, after anisotropic correction. Bottom) The grid-search carried out for the plunge and real percent of anisotropy related to upper layer. b) The same process applied in (a) is used here to estimate splitting parameters and plunge angle related to the lower layer, followed by anisotropic correction from upper layer.

synthetic receiver functions related to single- or multi-anisotropic layers. We observed that the aforementioned four-lobed pattern could be modified to an aligned pattern after anisotropic correction for the horizontal fast direction. But in the case of inclination of fast direction, the new two-lobed pattern was developed in the arrival times of the azimuthal Ps phases. We developed an empirical equation for this new two-lobed pattern. The plunge angle was estimated by forward modeling based on the method of Frederiksen and Bostock [18]. We applied this technique to real data relating to MOX and SHGR stations. The fast direction

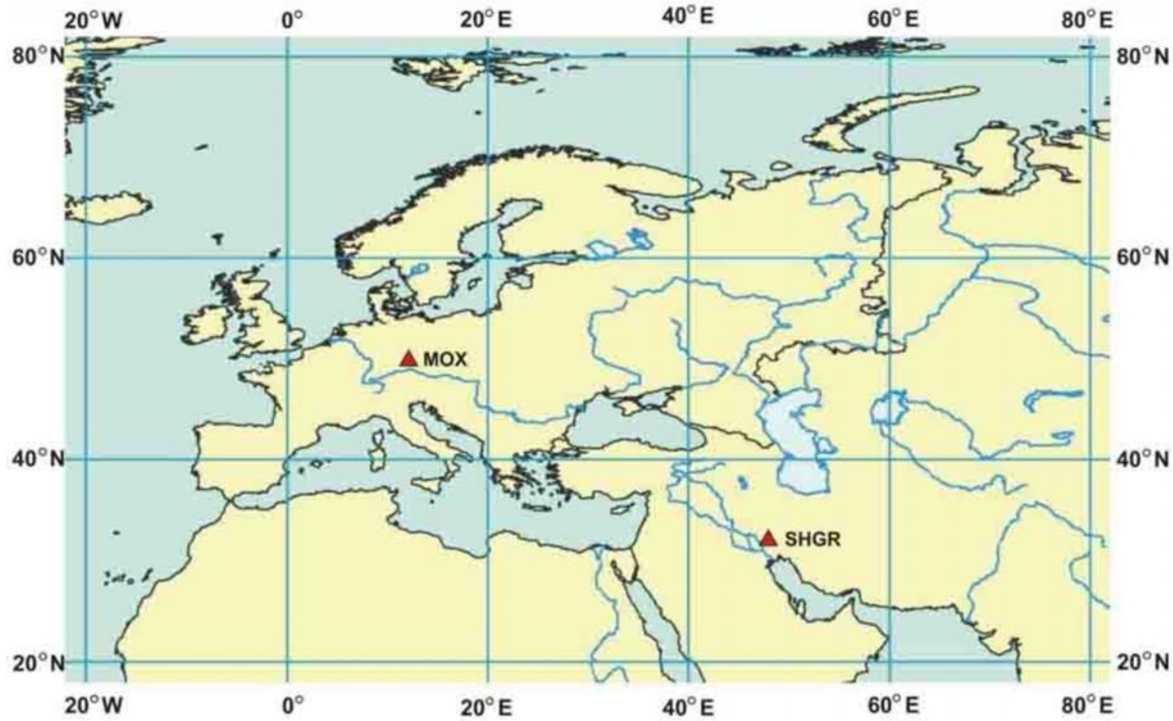

Figure 10. The SHGR and MOX stations located in southern Iran and Germany respectively.

Table 5. Results of forward modeling method for crustal anisotropic analysis related to SHGR and MOX stations.

Station	Thick. (km)	k (Vp/Vs)	¨ (deg)	Std ¨	plunge (sec)	Std plunge	true percent of anisotropy
SHGR	49.9	1.78	60	1	45	0.5	4.0%
MOX	32.7	1.7	98	2	45	0.2	5.5%

under the MOX station estimated in this study is relevant to the structure of the crust in Moxa region. Normally, the azimuth of fast axis in the crust should be parallel to the maximum principal stress direction [1]. According to Kasch et al. [20], the Moxa region is characterized by SW–NE trending folds. The maximum stress is normal to this direction which is parallel to fast direction estimated in Fig.12a. The fast direction inclination beneath the SHGR station was related to uppermost mantle which was coherent to the tectonic structure in this area [21, 22]. This technique is useful for evaluating the plunge effect on the actual anisotropy, and estimating the actual percentage of the anisotropy. Our study reveals that the magnitude of anisotropy, i.e. δt for the inclined fast axis was less than the horizontal fast axis. For example, the apparent split time in the crust of MOX station was 0.38 seconds, while the true percentage of anisotropy in this study had been measured to be 5.5%. Therefore, the true split time was estimated to be 0.47 seconds, which surpassed the apparent one. This phenomenon was due to the deviation of the fast direction from the horizontal.

The approximation of the plunge angle was very important in measuring the dip of layers in the studied area, however, it should be noted that the relation between the fast axis plunge and slop of the layer is not permanent. Deviation of the fast direction from horizontal may be a reason for the complication, however in some regions, it can be indicated as a subduction zone beneath the Moho discontinuity whereof the preferred lattice orientation of olivine crystals made an angel with the horizon. For example, there was an old subduction zone in the SHGR station which was located in south of the Zagros fold and thrust belt [21, 22]; this zone has been created by the northern margin of the Arabian plate colliding with the southern margin of the Eurasian plate. Therefore, the deviation from the horizontal is highly probable as regards the lattice preferred orientation of the crystals [12] — in the uppermost mantle — situated beneath the SHGR station. The fast direction plunge in the SHGR was almost consistent with the trend of ancient tectonics of the Zagros fold and thrust belt. The fast polarization direction in the discontinuity which actually exists

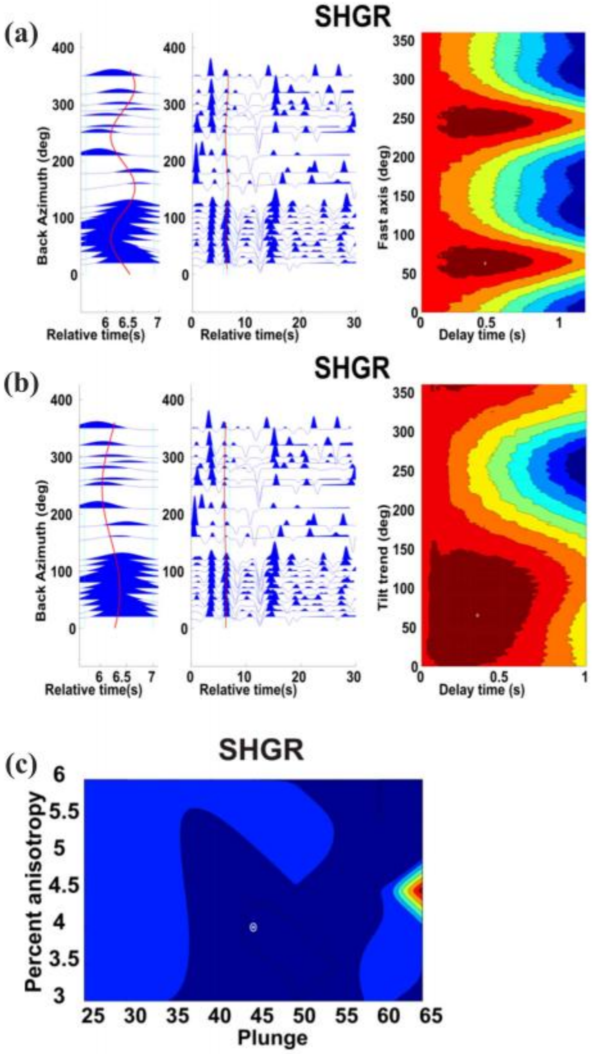

Figure 11. Application of the Ps splitting analysis and estimating plunge to data from the SHGR station of the Iranian National Seismic Network (INSN). a) The radial receiver functions of SHGR station are shown as a function of back-azimuth. The red line shows the harmonic pattern of Ps phases' arrival times and it is zoomed at left. The contour diagram shows splitting parameters relevant to discontinuity between crust and uppermost mantle beneath the SHGR station. b) The azimuthal receiver functions after anisotropic correction. The red cosine curve is the best-fitting curve to the maximum amplitudes of Ps phases. This curve have been estimated by stacking of maximum amplitudes which is fitted to this curve (it is shown in the right contour diagram). c) Grid-search carried out by forward modeling for the plunge and real percent of anisotropy.

beneath the Moho discontinuity was oriented NE-SW which was consistent with the converging zone between the Arabian and Eurasian plates.

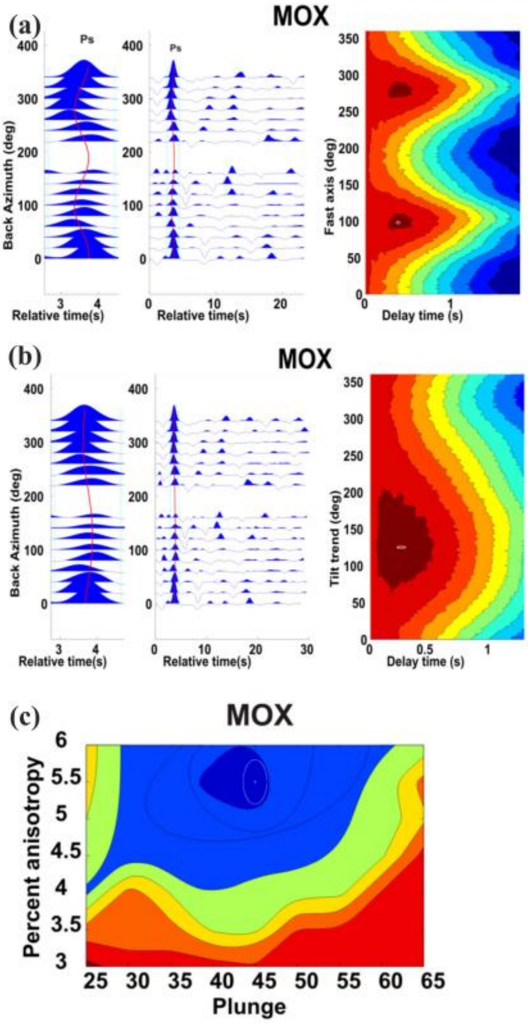

Figure 12. Application of the Ps splitting analysis and estimating plunge to data from the MOX station (Moxa) in Germany (Institute for Geosciences of the Friedrich-Schiller-University Jena, Burgweg). a) The radial receiver-functions of MOX station as a function of back azimuth. The red line shows the harmonic pattern of Ps phases arrival times and it is zoomed at left. The contour diagram shows splitting parameters relevant to discontinuity between crust and uppermost mantle beneath MOX station. b) The azimuthal receiver-functions after anisotropic correction. c) The grid-search carried out for the plunge and real percent of anisotropy using forward modeling.

Acknowledgments

We would like to thank two anonymous reviewers for their constructive and helpful comments. Many thanks to the "Iranian National Seismic Network (INSN)" and "Geophysik Uni Frankfurt - Goethe-Universität" for providing us with data we used in our analysis. We thank very much Dr. Georg Rümpker and

Dr. Ayoub Kaviani, former professors of K. Latifi, for providing us with some Matlab® codes which were used in this research.

References

1. Agard P., Omrani J., Jolivet L., Whitechurch H., Vrielynck B., Spakman W., Monié P., Meyer B., Wortel R. Zagros orogeny: a subduction-dominated process, Geological Magazine, 148. 692-725 (2011).
2. Audet P., Seismic anisotropy of subducting oceanic uppermost mantle from fossil spreading. *Geophys. Res. Lett.* **40**: 173–177 (2013).
3. Eckhardt C., Rabbel W. P receiver functions of anisotropic continental crust: A hierarchic catalogue of crustal models and azimuthal wave form patterns. *Geophys. J. Int.*, **187** (1): 439-479 (2011).
4. Fox O.C., Sheehan A.F. Upper Mantle Anisotropy Beneath Precambrian Province Boundaries, Southern Rocky Mountains. *American. Geophysical. Uni*. **10**: 1029, 1054GM26 (2005).
5. Frederiksen A.W., Bostock M.G. Modelling teleseismic waves in dipping anisotropic structures. *Geophys. J. Int.* **141:** 401-412 (2000).
6. Ito G., Dunn R, Li A, Wolfe C. J., Gallego A, and Fu Y. Seismic anisotropy and shear wave splitting associated with mantle plume-plate interaction, *J. Geophys. Res*. Solid Earth, **119**, doi: 10.1002/2013JB010735 (2014).
7. Kasch N., Naujoks M., Kley J., Jahr T. Combined geological and gravimetric mapping and modeling for an improved understanding of observed high-resolution gravity variations: a case study for the Global Geodynamics Project (GGP) station Moxa, Germany, *Int J Earth Sci (Geol Rundsch)*, doi: 10.1007/s00531-012-0859-z (2013).
8. Kaviani A., Hatzfeld D., Paul A, Tatar M., Priestley K. Shear-wave splitting, lithospheric anisotropy, and mantle deformation beneath the Arabia–Eurasia collision zone in Iran. *Earth and Planetary Science Letters*, **286** (3): 371-378 (2009).
9. Knoll M., Tommasi A., Loge R.E., Signorelli J.W. A multiscale approach to model the anisotropic deformation of lithospheric plates. *Geochem. Geophys. Geosyst.*, **10**: Q08009, doi:10.1029/2009GC002423 (2009).
10. Liu, H. & Niu, F. Estimating crustal seismic anisotropy with a joint analysis of radial and transverse receiver function data, *Geophys. J. Int*. **188**: 144–164 (2012).
11. McCormack K., Wirth, E.A., Long, M.D. B-type olivine fabric and mantle wedge serpentinization beneath the Ryukyu arc. *Geophys. Res. Lett*. **40**:1697-1702 (2013).
12. Nagaya M., Oda H., Akazawa H., Ishise M. Receiver functions of seismic waves in layered anisotropic media: application to the estimate of seismic anisotropy. *Bull. Seism. Soc. Am*. **98**: 2990- 3006 (2008).
13. Naus-Thijssen F. M. J., Goupee A. J., Vel S.S and Johnson S.E. The influence of microstructure on seismic wave speed anisotropy in the crust: computational analysis of quartz-muscovite rocks. *Geophys. J. Int.* **185** (2): 609-621 (2011).
14. Omrani, J., Agard, P., Whitechurch, H., Benoit, M., Prouteau, G., Jolivet, L. Arcmagmatism and subduction history beneath the Zagros Mountains, Iran: a new report of adakites and geodynamic consequences. *Lithos.* **106**: 380–398 (2008).
15. Paul A., Hatzfeld D., Kaviani A., Tatar M. & Pquegnat C. Seismic imaging of the lithospheric structure of the Zagros mountain belt Iran. *Geol. Soc. Lond. Special Publications.* **330**(1): 5–18 (2010).
16. Porter R., Zandt G., and McQuarrie N. Pervasive lower-crustal seismic anisotropy in Southern California: Evidence for underplated schists and active tectonics. Geological *Society of America, Lithosphere, published online.* doi:10.1130/L126.1. (2011).
17. Ribe N.M. Seismic anisotropy and mantle flow. *J. Geophys. Res*. **94**: 4213-4223 (1989).
18. Rümpker G., Kaviani A., Latifi K. Ps-splitting analysis for multilayered anisotropic media by azimuthal stacking and layer stripping. *Geophys, J. Int.* **199**(1):146-163 (2014).
19. Savage M.K. Seismic anisotropy and mantle deformation: What have we learned from shear wave splitting? *Reviews of Geophysics*. **37**(1): 65–106, doi: 10.1029/98RG02075 (1999).
20. Shearer P.M. Introduction to seismology, This Book published in the United States of America by Cambridge University *Press, New York* (2009).
21. Stein S., Wysession, M. An Introduction to seismology, Earthquakes, and Earth Structure. Blackwell Publishing, Oxford (2003).
22. Wenk H.R. Preferred Orientation in Deformed Metal and Rocks: An introduction to Modern Texture Analysis, This Book published in Department of Geology and Geophysics University of California Berkeley by *ACADEMIC PRESS, INC.* (1985).